Front. Optoelectron. 2012, 5(4): 429–434
DOI 10.1007/s12200-012-0293-7

RESEARCH ARTICLE

Flower-like CuO hierarchical nanostructures: synthesis, characterization, and property

Jiarui HUANG (✉), Feng TANG, Cuiping GU (✉), Chengcheng SHI, Muheng ZHAI

College of Chemistry and Materials Science, Anhui Normal University, Wuhu 241000, China

Abstract Nanoflake-based flower-like CuO nanostructures have been synthesized through thermal decomposition of $[Cu(NH_3)_4]^{2+}$ solution without any surfactants and catalysts at low temperature. The products are characterized by X-ray diffraction (XRD) and field-emission scanning electron microscopy (FESEM). The possible formation process based on the aggregation-recrystallization mechanism is proposed. Finally, the obtained flower-like CuO hierarchical nanostructures have been used as the photocatalyst in the experiments. It is found that the as-prepared flower-like CuO hierarchical nanostructures exhibit superior photocatalytic property on photocatalytic decomposition of Rhodamine B due to their hierarchical structures.

Keywords cupric oxide (CuO), microflowers, hierarchical nanostructures, photocatalytic property

1 Introduction

Controlled synthesis of inorganic nanostructures in terms of size and shape has been strongly motivated by their size and shape dependent properties and to achieve their desired practical applications [1–3]. Therefore, from the last decades, many efforts have been made to synthesized desired-shaped inorganic nanostructures with significantly improved physical and chemical properties for their possible applications in the fabrication of efficient devices [4,5]. Previously, three-dimensional (3D) nanostructures with complex morphology and high dimensionality have received great research interest due to the fact that their advanced geometric structure and atom arrangement on the specific facets of these nanostructures can provide novel properties [6–8]. Now, most of material scientists try their best to fabricate complex micro/nanoarchitectures and control the shape of nanostructures at the microscopic level.

As an important p-type semiconductor metal oxide with a narrow band gap, cupric oxide (CuO) is an exotic material both in terms of fundamental studies as well as practical applications. The excellent properties of CuO made it as a fantastic material for the diverse application, which includes heterogeneous catalysts, gas sensors, optical switch, magnetic storage media, lithium-ion electrode materials, field emission devices, solar cells, etc [9–13]. In addition to this, CuO-based materials are also well-known with regard to their high-temperature superconductivity and giant magnetoresistance [14,15]. Thus, due to various properties and vast applications, variety of CuO nanostructures, such as nanorods, nanowires, nanosheets, etc., have been fabricated by a range of fabrication techniques and reported in the literature [9–15]. In recent years, the synthesis and structural properties of complex CuO nanostructures, such as flower-shaped nanostructures [16–18], hollow microspheres [8,19], nanorod bundles [20], urchin-like microspheres [21], also have been reported in the literature. For example, Wang et al. have founded a chemical method to synthesize complex CuO nanostructures and determined the photocatalytic activity [8]. Basu et al. reported that monoclinic CuO nanofloweres on resin support were used as recyclable catalyst to obtain perylene compound [16]. Wang et al. presented the composite-hydroxide-mediated and the composite-molten-salt synthesis methods for the preparation of flower-like and rod-shaped CuO nanostructures, during the experiment they used many chemical reagents [22]. It can be seen from the previous reports that the conventional methods for preparing complex CuO nanostructures usually require higher temperature, pressure and longer reaction time. Therefore, it is still needed to develop a simple and effective method to synthesized complex CuO nanostructures in large-quantity at low temperature and short time.

In this paper, we present a facile and green method for synthesis of nanoflake-based flower-like CuO hierarchical

Received September 12, 2012; accepted September 20, 2012

E-mail: jrhuang@mail.ahnu.edu.cn, cpgu2008@mail.ahnu.edu.cn

nanostructures through thermal decomposition of $[Cu(NH_3)_4]^{2+}$ solution without any surfactants and catalysts at low temperature. On the basis of the evolution of the structure and the morphology with the increase of the reaction time, the possible growth mechanism of CuO hierarchical nanostructures is proposed. Furthermore, the photocatalytic property of the flower-like CuO hierarchical nanostructures is also investigated.

2 Experimental details

2.1 Synthesis of samples

All of the chemical reagents were analytic grade and were used as received without further purification. A typical synthesis procedure of the flower-like CuO nanostructures was as follows: 1.0 g of copper nitrate trihydrate ($Cu(NO_3)_2 \cdot 3H_2O$) was dissolved in 30 mL distilled water under vigorous stirring, followed by addition of 7.0 mL ammonia ($NH_3 \cdot H_2O$, $3.5\,mol \cdot L^{-1}$) to form blue solution. After that, the beaker was sealed with cleaning wrap, maintained at 80°C for 4 h. Subsequently, the black precipitates on the wall of the beaker were washed with distilled water and absolute ethanol several times to remove the impurities.

2.2 Characterization

The products were characterized by X-ray diffraction (XRD, Shimadzu XRD-6000, with high-intensity Cu *Kα* radiation, wavelength 1.54178 Å), and field-emission scanning electron microscopy (FE-SEM, Hitachi S-4800, operated at 5 kV).

2.3 Photocatalysis measurement

The photocatalytic experiments were carried out by adding 20 mg of photocatalyst into 50 mL Rhodamine B aqueous solution with the concentration of 10 mg/L. The suspension was ultrasonicated for 30 min, and then stirred for another 30 min in dark to obtain adsorption equilibrium of dye molecules before illumination. Then, the suspension was irradiated with a 365 nm UV light (Philips, 300 W). During the full irradiation process, the suspension was stirred continuously. At a given time interval, 4 mL of suspension was taken out and immediately centrifuged to eliminate the solid particles. The absorbance of the filtrate was measured by a Hitachi U-3010 UV-vis absorption spectrophotometer (Tokyo, Japan) at the maximum absorbance peak (554 nm).

3 Results and discussion

3.1 Structure and morphology

Figure 1 is the XRD pattern of the product prepared under the present experimental conditions. All peaks can be indexed as monoclinic CuO phase by comparison with the JCPDS card files no. 48–1548. No other impurity peaks are detected, indicating that the product is rather pure.

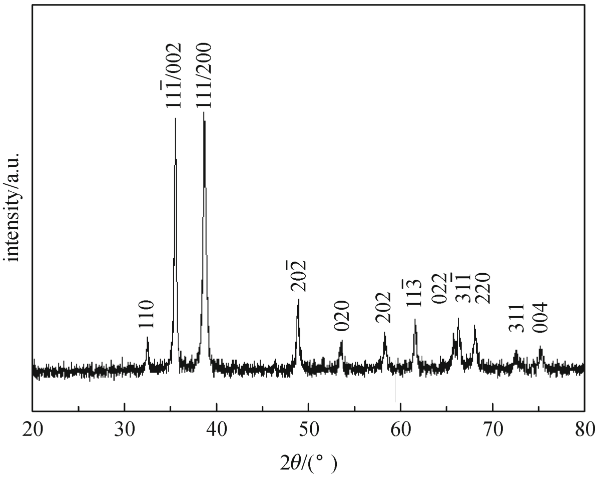

Fig. 1 XRD pattern of as-prepared product

The SEM images of the as-prepared CuO products are shown in Fig. 2. Figures 2(a) and 2(b) are the images of the CuO microflowers in low magnification and medium magnification, respectively. From the SEM observations, the CuO product consists of numerous flower-like aggregates with multi-leaves, and almost all of them show the same morphology. The CuO microflowers have diameters of approximate 3–4 μm. As shown in Fig. 2(b), the microflower is composed of numerous thin nanoflakes. Careful examination reveals that the thickness of the nanoflakes is ca. 15 nm. Furthermore, each nanoflake has almost the same thickness perpendicular to its 2D face, indicating that the plate growth is strictly extended in the 2D plane throughout the whole growing process. To give a further understanding of these CuO microflowers, the sample was intensively sonicated for 5 min in ethanol. Most of CuO microflowers and little individual nanoflakes (most of the nanoflakes connected together and could not be moved off by the sonication) can be observed in the sonicated sample.

3.2 Discussion on growth mechanism

To reveal the formation process of the flower-like CuO hierarchical nanostructures in detail, time-dependent experiments were carried out and the resultant products were analyzed by SEM. The typical images of the products prepared at certain reaction time intervals are shown in Fig. 3. Figure 3(a) shows that a large number of particles can be obtained on the glass substrate in a short time of 15 min under the present condition. When the reaction time reaches 0.5 h, the SEM observation (shown in Fig. 3(b)) reveals that there are some small microflowers scattered on the glass surface. When the reaction time is increased to

1.5 h, some large hierarchical flower-like structures are produced as shown in Fig. 3(c). At the same time, the nanoparticles and the small particles disappear from glass surface. When the reaction time is prolonged to 4 h, a large number of fully developed flower-like hierarchical nanostructures are observed (shown in Fig. 2(a)).

$$[\mathrm{Cu(NH_3)_4}]^{2+} + \mathrm{H_2O} = \mathrm{CuO} \downarrow + 2\mathrm{NH_3} + 2\mathrm{NH_4^+} \quad (1)$$

On the basis of the above experimental results, the formation of the flower-like hierarchical nanostructures may be attributed to the Ostwald ripening process, which has been researched intensively by many researchers recently [23,24]. Here, we propose a possible schematic representation for the formation of the flower-like hierarchical nanostructures, as described in Fig. 4. In the initial reaction stage, CuO nucleus obtained through the thermal decomposition of $[\mathrm{Cu(NH_3)_4}]^{2+}$ solution, as Eq. (1) depicted, tends to form the aggregated CuO particles on the glass substrate to minimize the overall energy of the system (step 1). In this step, these primary CuO nanoparticles are metastable due to their high surface energy. As the reaction proceeded, more and more new nucleus kept forming and then aggregated on the particles of the glass substrate. When there are no structure-directing chemicals, the as-formed nanoparticles are of monoclinic nature and these monoclinic particles aggregate to form CuO nanoflakes. Therefore, a large number of nanoflakes even some small microflowers on the glass substrate are formed during this process (step 2). As the reaction went on, some new nucleus kept forming and then aggregated on the nanoflakes to form the microflowers (step 3). From the thermodynamics point of view, the surface energy of an individual nanoflake is quite high with two main exposed planes, and thus they tend to aggregate and decrease the surface energy by reducing exposed areas. The surface energy is substantially reduced when the neighboring nanoflakes are grown. Furthermore, during the recrystallization procedure, the CuO nanoparticles and small nanoflakes with high surface energy decompose and recrystallize. In the subsequent crystal growth process, the nanoparticles and small nanoflakes can be completely consumed and the fully developed CuO microflowers with closely arranged thin nanoflakes are fabricated. During the whole formation process, we estimated that $\mathrm{NH_3 \cdot H_2O}$ not only decreases the formation rate of CuO nucleus, but also plays a role as additives which can connect nanoflakes to microflowers.

3.3 Photocatalysis properties of flower-like CuO hierarchical nanostructures

To evaluate the photocatalytic activity of our products, we measured the optical property changes of Rhodamine B aqueous solution in the presence of flower-like CuO hierarchical nanostructures under the irradiation of the 365 nm UV light for given time, respectively. The time-dependent absorption spectra of Rhodamine B solution containing flower-like CuO hierarchical nanostructure catalyst during the irradiation are illustrated in Fig. 5(a). It can be seen that the maximum absorbance at 554 nm decreases rapidly with irradiation time as shown in Fig. 5(a). The absorption intensity of the peak was reduced by approximate 26% when the solution had been irradiated under 365 nm UV light for 15 min in the presence of flower-like CuO hierarchical nanostructures. While after it had been irradiated under 365 nm UV light for 105 min, its absorption peak disappeared almost completely, indicating that most amount of Rhodamine B was degraded. The decoloration of solution can be due to the destruction of the dye chromogen. Since no new absorption peak is observed,

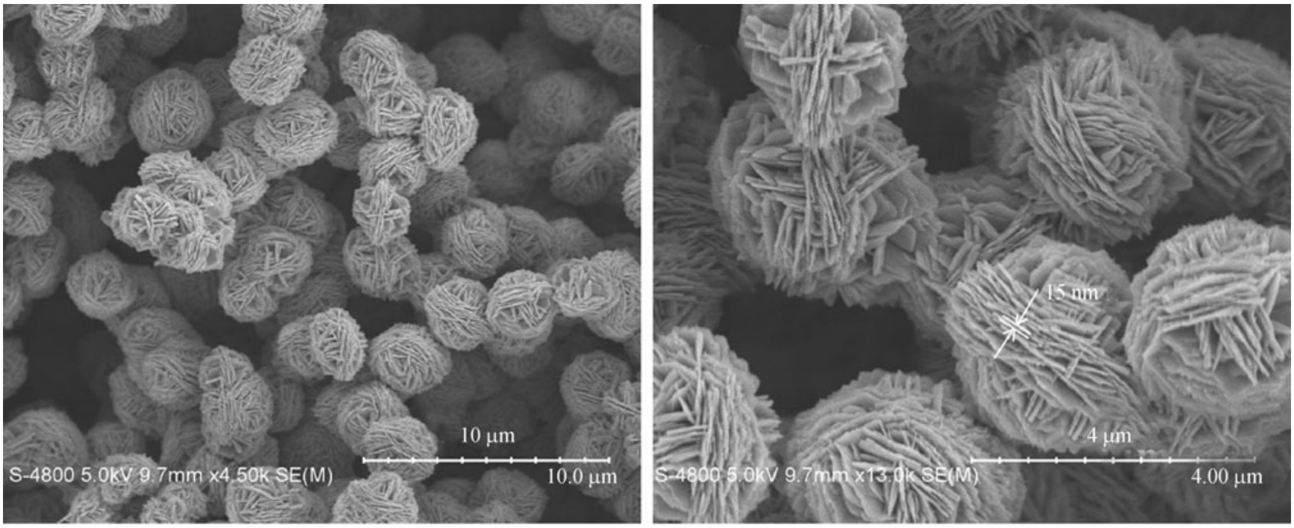

(a) (b)

Fig. 2 (a) and (b) SEM images of as-precipitates obtained through thermal decomposition of $[\mathrm{Cu(NH_3)_4}]^{2+}$ solution

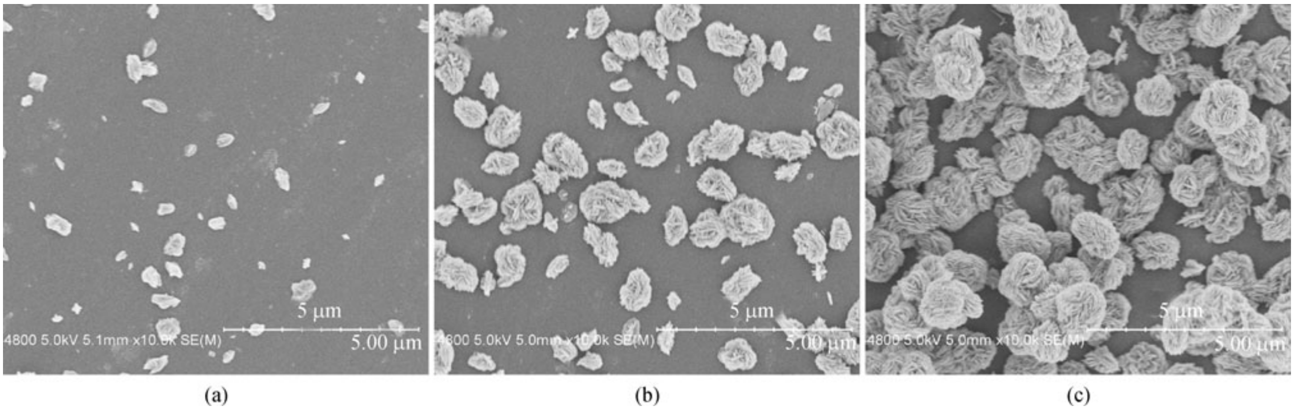

Fig. 3 SEM images of as-precipitates obtained through thermal decomposition of $[Cu(NH_3)_4]^{2+}$ solution obtained after hydrothermal reaction at 80°C for (a) 15 min; (b) 0.5 h; (c) 1.5 h

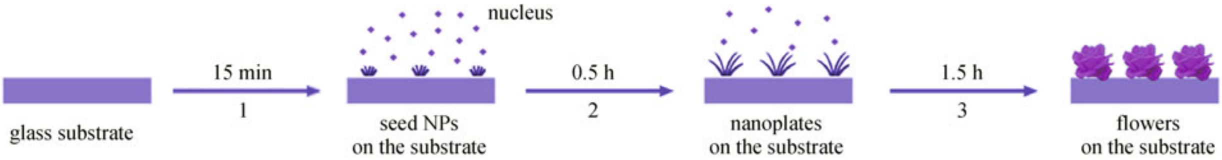

Fig. 4 Schematic illustration of formation process and shape evolution of flower-like CuO hierarchical nanostructures

the Rhodamine B has been decomposed [8]. Significantly, the absorption peak intensity slightly decreases after the solution containing Pyronine B is irradiated by 365 nm UV light for 105 min in the absence of any CuO particles, which reveals the obvious photocatalytic ability of CuO. The fitting of absorbance maximum plot versus time indicates an exponential decay as shown in Fig. 5(a) (insert). The normalized concentration of the solution equals the normalized maximum absorbance, so we use C_0/C to take place of A_0/A, where C_0 and C are the initial and actual concentration of Rhodamine B, respectively. It has been already proved that the photocatalytic decomposition of Rhodamine B solution agrees with pseudo-first-order kinetics [25–27]. As a result, the rate constants (k) can be calculated by the equation: $\ln(C/C_0) = -kt$. As seen in Fig. 5(a), the quantity $\ln(C_0/C)$ is plotted as a function of irradiation times to calculate the photocatalytic reaction rate constant. The photocatalytic reaction rate constants of the flower-like CuO hierarchical nanostructures under UV light are calculated as 0.033 min^{-1}. The as prepared flower-like CuO hierarchical nanostructures show higher effective photocatalytic property for the direct degradation of Rhodamine B than CuO hollow microspheres [8].

The photocatalytic properties in the degradation of Rhodamine B of the flower-like CuO hierarchical nanostructures suggest that the as-prepared flower-like CuO hierarchical nanostructures have potential application in water treatment. In general, organic dye solutions irradiated by UV light can produce hydroxyl radicals, which lead to structural changes in dyes [28]. As a result, the optical properties of the dyes will change. Pyronine B is an ionic compound dye. After it had been irradiated under 365 nm UV light for 15 min, its absorption peak slightly decreased, indicating that only little amount of Pyronine B was degraded (data not shown). Namely, its activation energy of the photodegradation reaction was higher in the absence of catalysts. After flower-like CuO hierarchical nanostructures were introduced to the solution of Pyronine B, an intermediary could be produced owing to the electrostatic interaction between flower-like CuO hierarchical nanostructures and Pyronine B. Since CuO is a p-type semiconductor with the band gap of 1.7 eV [29], it can easily produce electron-hole pairs under the UV irradiation, which rapidly transfer into hydroxyl radicals in the solution. As a result, the photocatalytic degradation of Pyronine B was promoted. The above process is simply illustrated in Fig. 5(b). It is generally accepted that the catalytic process is mainly related to the adsorption and desorption of molecules on the surface of the catalyst. The hierarchical structures in the catalyst enable storage of more molecules. Therefore, the nanoflake-based hierarchical structure nature provides more active reaction sites, which promote photocatalytic activity of CuO [30].

4 Conclusions

In summary, flower-like CuO hierarchical nanostructures have been synthesized through thermal decomposition of $[Cu(NH_3)_4]^{2+}$ solution without any surfactants and cata-

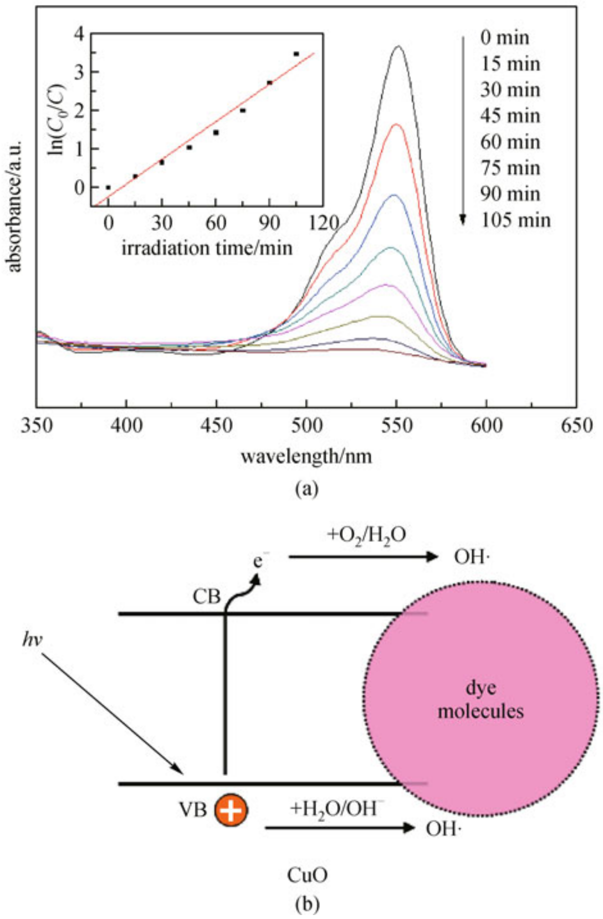

Fig. 5 (a) Absorption spectrum and photodecomposition of Rhodamine B solution (10 mg/L, 50 mL) in presence of flower-like CuO hierarchical nanostructures under UV irradiation. Insets are the photodegradation plots of Rhodamine B under UV-light, in which C is the concentration of Rhodamine B and C_0 is the initial concentration; (b) simplified scheme of Pyronine B photodegradation under irradiation of 365 nm UV light in presence of CuO

lysts at low temperature. The possible formation process based on the aggregation-recrystallization mechanism is proposed. $NH_3 \cdot H_2O$ not only decreases the formation rate of CuO nucleus, but also plays a role as additives which can connect nanoflakes to nanoflowers. The as-synthesized flower-like CuO hierarchical nanostructures are good photocatalysts for degradation of some organic dyes due to their hierarchical structures, which have potential applications in the treatment of waste water and the protection of environment.

Acknowledgements This work was supported by the National Natural Science Foundation of China (Grant Nos. 21105001and 61203212), and Anhui Provincial Natural Science (No. 10040606Q34).

References

1. Huo Y J, Lin H, Chen R, Rong Y W, Kamins T I, Harris J S. MBE growth of tensile-strained Ge quantum wells and quantum dots. Frontiers of Optoelectronics, 2012, 5(1): 112–116
2. Xue F, Liu F, Huang Y D. Spontaneous emission rate enhancement of nano-structured silicon by surface plasmon polariton. Frontiers of Optoelectronics, 2012, 5(1): 51–62
3. Gowda S R, Reddy A L M, Shaijumon M M, Zhan X B, Ci L J, Ajayan P M. Conformal coating of thin polymer electrolyte layer on nanostructured electrode materials for three-dimensional battery applications. Nano Letters, 2011, 11(1): 101–106
4. Ewers T D, Sra A K, Norris B C, Cable R E, Cheng C H, Shantz D F, Schaak R E. Spontaneous hierarchical assembly of rhodium nanoparticles into spherical aggregates and superlattices. Chemistry of Materials, 2005, 17(3): 514–520
5. Liu W T. Nanoparticles and their biological and environmental applications. Journal of Bioscience and Bioengineering, 2006, 102 (1): 1–7
6. Jin D L, Miu X, Yu X J, Wang L N, Wang N Y, Wang L C. Synthesis of core-shell microspheres of poly(methyl methacrylate)-CuO by solution deposition method. Materials Chemistry and Physics, 2010, 124(1): 69–72
7. Yu L G, Zhang G M, Wu Y, Bai X, Guo D Z. Cupric oxide nanoflowers synthesized with a simple solution route and their field emission. Journal of Crystal Growth, 2008, 310(12): 3125–3130
8. Wang S L, Xu H, Qian L Q, Jia X, Wang J W, Liu Y Y, Tang W H. CTAB-assisted synthesis and photocatalytic property of CuO hollow microspheres. Journal of Solid State Chemistry, 2009, 182 (5): 1088–1093
9. Switzer J A, Kothari H M, Poizot P, Nakanishi S, Bohannan E W. Enantiospecific electrodeposition of a chiral catalyst. Nature, 2003, 425(6957): 490–493
10. Chowdhuri A, Gupta V, Sreenivas K, Kumar R, Mozumdar S, Patanjali P K. Response speed of SnO_2-based H_2S gas sensors with CuO nanoparticles. Applied Physics Letters, 2004, 84(7): 1180–1182
11. Gao X P, Bao J L, Pan G L, Zhu H Y, Huang P X, Wu F, Song D Y. Preparation and electrochemical performance of polycrystalline and single crystalline CuO nanorods as anode materials for Li ion battery. Journal of Physical Chemistry B, 2004, 108(18): 5547–5551
12. Hsieh C T, Chen J M, Lin H H, Shih H C. Field emission from various CuO nanostructures. Applied Physics Letters, 2003, 83(16): 3383–3385
13. Chen J, Deng S Z, Xu N S, Zhang W X, Wen X G, Yang S H. Temperature dependence of field emission from cupric oxide nanobelt films. Applied Physics Letters, 2003, 83(4): 746–748
14. Wen X G, Xie Y T, Choi C L, Wan K C, Li X Y, Yang S H. Copper-based nanowire materials: templated syntheses, characterizations, and applications. Langmuir, 2005, 21(10): 4729–4737
15. Liu Y, Chu Y, Li M Y, Li L L, Dong L H. In situ synthesis and assembly of copper oxide nanocrystals on copper foil via a mild hydrothermal process. Journal of Materials Chemistry, 2006, 16(2): 192–198
16. Basu M, Sinha A K, Pradhan M, Sarkar S, Pal A, Pal T. Monoclinic CuO nanoflowers on resin support: recyclable catalyst to obtain perylene compound. Chemical Communications (Cambridge), 2010, 46(46): 8785–8787
17. Gu A X, Wang G F, Zhang X J, Fang B. Synthesis of CuO

nanoflower and its application as a H_2O_2 sensor. Bulletin of Materials Science, 2010, 33(1): 17–20

18. Yang Z H, Xu J, Zhang W X, Liu A P, Tang S P. Controlled synthesis of CuO nanostructures by a simple solution route. Journal of Solid State Chemistry, 2007, 180(4): 1390–1396
19. Yang S Y, Wang C F, Chen L, Chen S. Facile dicyandiamide-mediated fabrication of well-defined CuO hollow microspheres and their catalytic application. Materials Chemistry and Physics, 2010, 120(2–3): 296–301
20. Yang L X, Zhu Y J, Tong H, Li L, Zhang L. Multistep synthesis of CuO nanorod bundles and interconnected nanosheets using $Cu_2(OH)_3Cl$ plates as precursor. Materials Chemistry and Physics, 2008, 112(2): 442–447
21. Hong J M, Li J, Ni Y H. Urchin-like CuO microspheres: Synthesis, characterization, and properties. Journal of Alloys and Compounds, 2009, 481(1–2): 610–615
22. Wang X, Hu C G, Liu H, Du G J, He X S, Xi Y. Synthesis of CuO nanostructures and their application for nonenzymatic glucose sensing. Sensors and Actuators B, Chemical, 2010, 144(1): 220–225
23. Lou X W, Li C M, Archer L A. Designed synthesis of coaxial SnO_2@carbon hollow nanospheres for highly reversible lithium storage. Advanced Materials (Deerfield Beach, Fla.), 2009, 21(24): 2536–2539
24. Yin X M, Li C C, Zhang M, Hao Q Y, Liu S, Chen L B, Wang T H. One-step synthesis of hierarchical SnO_2 hollow nanostructures via self-assembly for high power lithium ion batteries. Journal of Physical Chemistry C, 2010, 114(17): 8084–8088
25. Bayati M R, Golestani-Fard F, Moshfegh A Z. Visible photodecomposition of methylene blue over micro arc oxidized WO_3-loaded TiO_2 nano-porous layers. Applied Catalysis A: General, 2010, 382(2): 322–331
26. Bayati M R, Moshfegh A Z, Golestani-Fard F. On the photocatalytic activity of the sulfur doped titania nano-porous films derived via micro-arc oxidation. Applied Catalysis A: General, 2010, 389(1–2): 60–67
27. Houas A, Lachheb H, Ksibi M, Elaloui E, Guillard C, Herrmann J M. Photocatalytic degradation pathway of methylene blue in water. Applied Catalysis B: Environmental, 2001, 31(2): 145–157
28. Hoffmann M R, Martin S T, Choi W, Bahnemannt D W. Environmental applications of semiconductor photocatalysis. Chemical Reviews, 1995, 95(1): 69–96
29. Jiang H Q, Endo H, Natori H, Nagai M, Kobayshi K. Fabrication and efficient photocatalytic degradation of methylene blue over $CuO/BiVO_4$ composite under visible-light irradiation. Materials Research Bulletin, 2009, 44(3): 700–706
30. Li H X, Bian Z F, Zhu J, Zhang D Q, Li G, Huo Y, Li H, Lu Y. Mesoporous titania spheres with tunable chamber stucture and enhanced photocatalytic activity. Journal of the American Chemical Society, 2007, 129(27): 8406–8407